



OPEN

Effect of teriparatide on drug treatment of tuberculous spondylitis: an experimental study

Subum Lee¹, Ye-Jin Seo², Je-Yong Choi³, Xiangguo Che³, Hyun-Ju Kim³, Seok-Yong Eum⁴, Min-Sun Hong⁴, Sun-Kyoung Lee⁴ & Dae-Chul Cho²✉

Tuberculous spondylitis often develops catastrophic bone destruction with uncontrolled inflammation. Because anti-tuberculous drugs do not have a role in bone formation, a combination drug therapy with a bone anabolic agent could help in fracture prevention and promote bone reconstruction. This study aimed to investigate the influence of teriparatide on the effect of anti-tuberculous drugs in tuberculous spondylitis treatment. We used the virulent *Mycobacterium tuberculosis* (Mtb) H37Rv strain. First, we investigated the interaction between teriparatide and anti-tuberculosis drugs (isoniazid and rifampin) by measuring the minimal inhibitory concentration (MIC) against H37Rv. Second, we evaluated the therapeutic effect of anti-tuberculosis drugs and teriparatide on our previously developed in vitro tuberculous spondylitis model of an Mtb-infected MG-63 osteoblastic cell line using acid-fast bacilli staining and colony-forming unit counts. Selected chemokines (interleukin [IL]-8, interferon γ -induced protein 10 kDa [IP-10], monocyte chemoattractant protein [MCP]-1, and regulated upon activation, normal T cell expressed and presumably secreted [RANTES]) and osteoblast proliferation (alkaline phosphatase [ALP] and alizarin red S [ARS] staining) were measured. Teriparatide did not affect the MIC of isoniazid and rifampin. In the Mtb-infected MG-63 spondylitis model, isoniazid and rifampin treatment significantly reduced Mtb growth, and cotreatment with teriparatide did not change the anti-tuberculosis effect of isoniazid (INH) and rifampin (RFP). IP-10 and RANTES levels were significantly increased by Mtb infection, whereas teriparatide did not affect all chemokine levels as inflammatory markers. ALP and ARS staining indicated that teriparatide promoted osteoblastic function even with Mtb infection. Cotreatment with teriparatide and the anti-tuberculosis drugs activated bone formation (ALP-positive area increased by 705%, $P=0.0031$). Teriparatide was effective against Mtb-infected MG63 cells without the anti-tuberculosis drugs (ARS-positive area increased by 326%, $P=0.0037$). Teriparatide had no effect on the efficacy of anti-tuberculosis drugs and no adverse effect on the activity of Mtb infection in osteoblasts. Furthermore, regulation of representative osteoblastic inflammatory chemokines was not changed by teriparatide treatment. In the in vitro Mtb-infected MG-63 cell model of tuberculous spondylitis, cotreatment with the anti-tuberculosis drugs and teriparatide increased osteoblastic function.

Globally, an estimated 10 million people contracted tuberculosis in 2019¹ and the proportion of extrapulmonary tuberculosis cases is increasing in developed countries². Tuberculous spondylitis accounts for 1–5% of tuberculosis cases and represents ~50% of all bone and joint tuberculosis³. Compared to bacterial spondylitis, the diagnosis of tuberculous spondylitis is often delayed, and the worst complications, spinal deformities with bone destruction and neurological deficits, often follow⁴. Despite advances in diagnostic techniques, even in developed countries, neurological deficits are still present at the time of diagnosis in 45% of the cases⁵.

As anti-tuberculosis drugs are long-term drugs, external immobilization and bed rest are the conventional recommendations for patients with tuberculous spondylitis with pathological fracture. However, treatment with only anti-tuberculosis medications for an extended period of up to 1 year is an inadequate strategy to address

¹Department of Neurosurgery, Korea University Anam Hospital, Korea University College of Medicine, Seoul, Republic of Korea. ²Department of Neurosurgery, School of Medicine, Kyungpook National University, Kyungpook National University Hospital, 130 Dongduk-Ro, Jung-Gu, Daegu, Republic of Korea. ³Department of Biochemistry and Cell Biology, School of Medicine, Kyungpook National University, Daegu, Republic of Korea. ⁴Division of Immunopathology and Cellular Immunology, International Tuberculosis Research Center, Gyeongsangnam-Do, Changwon-Si, Republic of Korea. ✉email: dccho@knu.ac.kr

* INH + RFP

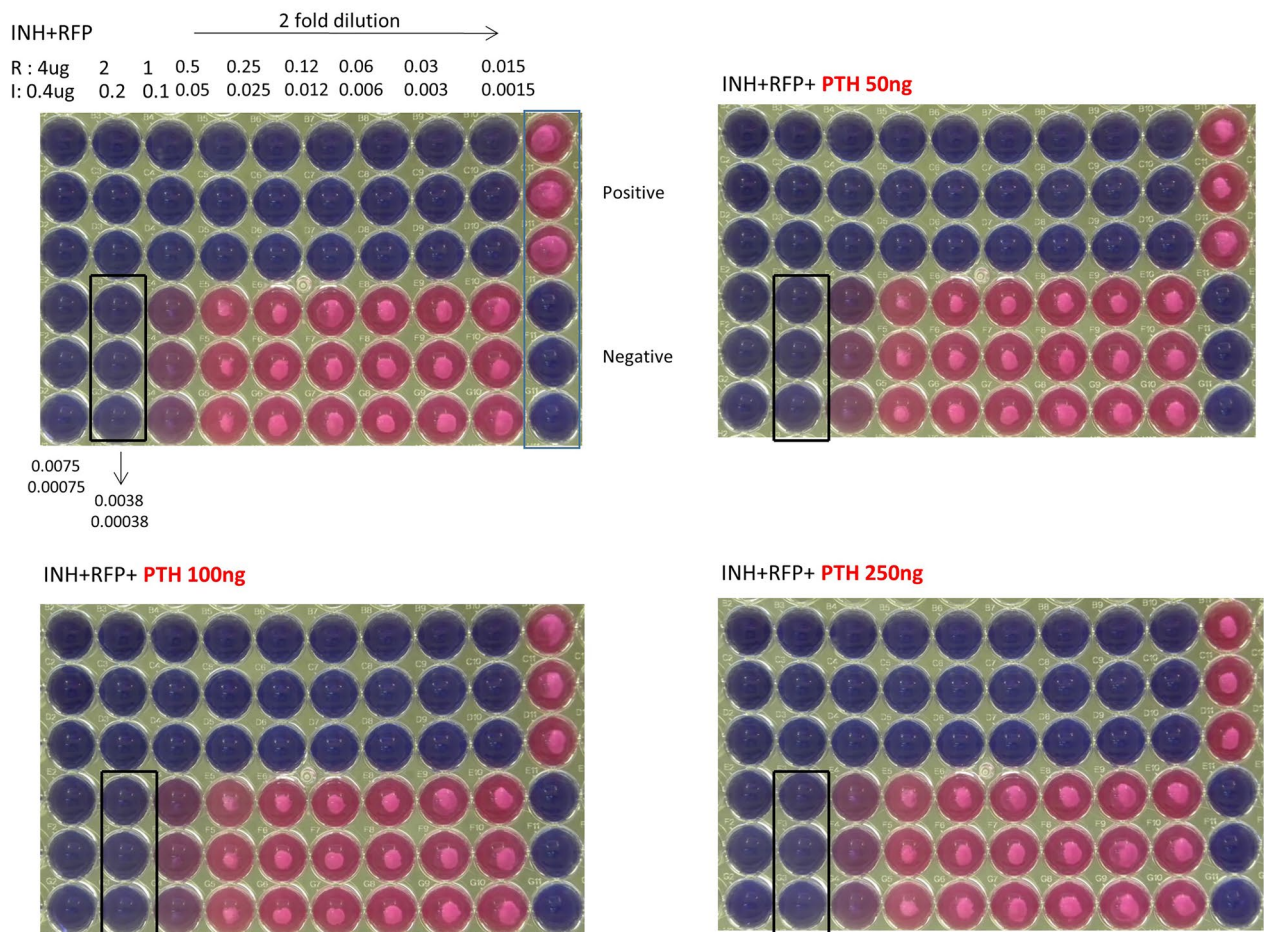


Figure 1. Minimum inhibitory concentration (MIC) assay of isoniazid plus rifampicin (INH + RFP) according to various teriparatide concentration (0, 50, 100, and 250 ng). Abbreviations: INH, isoniazid; PTH, teriparatide; RFP, rifampin.

the catastrophic bone destruction. Furthermore, concurrent spinal surgery such as screw fixation and bone fusions still lead to poor surgical outcomes compared with that of general spinal surgery because of osteolysis and deterioration of bone formation due to inflammation⁶.

Therefore, traditional anti-tuberculosis agents may need to be combined with drugs that minimize the destruction of vertebrae and promote osseointegration to effectively treat tuberculosis infection. To fill this therapeutic gap, teriparatide, a recombinant human parathyroid hormone (PTH), could be considered as an optimal combination as an anabolic agent. However, no studies have been conducted on the safety and efficacy of teriparatide in patients who require anti-tuberculosis treatment.

Based on previous studies, teriparatide is recognized to be contraindicated in osteosarcoma or malignant melanoma because it could cause disease progression^{7,8}, but to the best of our knowledge, its propensity to cause a similar problem in tuberculosis has not been determined. Minimal evidence for considering the clinical use of teriparatide for tuberculous spondylitis would come from the verification of two required characteristics. Teriparatide must not interfere with the action of anti-tuberculosis drugs and should not increase the rate of *Mycobacterium tuberculosis* (Mtb) infection; in the present study, we aimed to obtain experimental evidence to confirm that teriparatide meets the two requirements. Furthermore, we established an in vitro spondylitis model to evaluate whether the anabolic activity of teriparatide mediates its effects on Mtb-infected osteoblasts.

Results

Drug interaction: anti-tuberculosis drugs and teriparatide. The MICs of INH and RFP against the Mtb strain were confirmed to be 0.0038 and 0.00038 µg/mL, respectively, both alone and following cotreatment with teriparatide 50, 100, and 250 ng/mL (Fig. 1), indicating that teriparatide (0–250 ng/mL) showed no concentration-dependent effect.

FACS (MFI)	H37Rv					H37Rv + PTH					H37Rv + INH + RFP					H37Rv + INH + RFP + PTH						
MFI	1	2	3	AVE	SEM	1	2	3	AVE	SEM	1	2	3	AVE	SEM	1	2	3	AVE	SEM		
Day 0	13.55	15.26	16	14.9	0.7	13.55	15.26	16	14.9	0.7	13.55	15.26	16	14.9	0.7	13.55	15.26	16	14.9	0.7		
Day 1	29.81	30.26	34.36	31.5	1.4	32.91	29.14	27.78	29.9	1.5	12.78	11.97	12.03	12.3	0.3	13.23	11.64	10.71	11.9	0.7		
Day 4	46.05	45.21	44.79	45.4	0.4	39.6	38.28	40.43	39.4	0.6	4.48	6.33	7.64	6.2	0.9	6.52	7.49	7.4	7.1	0.3		
Day 7	95.51	97.36	81.15	91.3	5.1	105.41	96.46	99	100.3	2.7	4.11	4.47	3.2	3.9	0.4	4.14	3.55	3.93	3.9	0.2		
CFU	H37Rv										H37Rv + PTH											
($\times 10^6$ cells)	1	2	3	4	5	6	7	8	9	AVE	SEM	1	2	3	4	5	6	7	8	9	AVE	SEM
Day 0	2.6	1.7	3.3	5.4	4.6	2.6	6	4.4	4.4	3.9	0.5	2.6	1.7	3.3	5.4	4.6	2.6	6	4.4	4.4	3.9	0.5
Day 1	10.2	9.2	10	8.8	9.2	10	6.4	15.2	8.8	9.8	0.8	7.2	6	9.2	9.2	7.2	11.2	10.4	10.4	10.4	9.0	0.6
Day 4	26.4	26.8	24.4	29.6	22.4	16.8	31.2	25.2	22.8	25.1	1.4	14.4	18.4	20	20.8	16	22.4	20.4	10.8	9.6	17.0	1.5
Day 7	52	51.2	35.2	34.8	37.2	31.2	27	31.5	22.5	35.8	3.3	20	42.4	30.4	37.2	43.2	33.6	30	30	36	33.6	2.4
CFU	H37Rv + INH + RFP										H37Rv + INH + RFP + PTH											
($\times 10^6$ cells)	1	2	3	4	5	6	7	8	9	AVE	SEM	1	2	3	4	5	6	7	8	9	AVE	SEM
Day 0	2.6	1.7	3.3	5.4	4.6	2.6	6	4.4	4.4	3.9	0.5	2.6	1.7	3.3	5.4	4.6	2.6	6	4.4	4.4	3.9	0.5
Day 1	1.95	1.85	1.95	4	4.1	3.7	1.8	1.4	2.4	2.6	0.4	1.6	1.85	1.9	2.3	1.9	3.4	1	2.4	2.4	2.1	0.2
Day 4	0.188	0.203	0.224							0.2	0.0	0.1	0.076	0.141							0.1	0.0
Day 7	0.0264	0.0238	0.024	0.0535	0.044	0.0485				0.0	0.0	0.0118	0.0114	0.014	0.0215	0.02	0.026				0.0	0.0

Table 1. Mean fluorescence intensity (MFI) and colony-forming units (CFU) results.

Effects of teriparatide on Mtb activity. The results of the MFI and CFU evaluation of MG-63 cells infected with Mtb H37Rv and cultured for 7 days showed that the number of infecting Mtb bacilli significantly increased, from day 0 to day 7 (Table 1). Treatment with the anti-tuberculosis drugs eradicated the Mtb infection. Figure 2 shows the infection and growth of Mtb in MG63 cells during the in vitro tuberculous spondylitis model establishment. The results showed that cotreatment with teriparatide (50 ng/mL) did not adversely affect the anti-tuberculosis activity of INH or RFP, which showed no change in activity against Mtb (Table 1, Fig. 2).

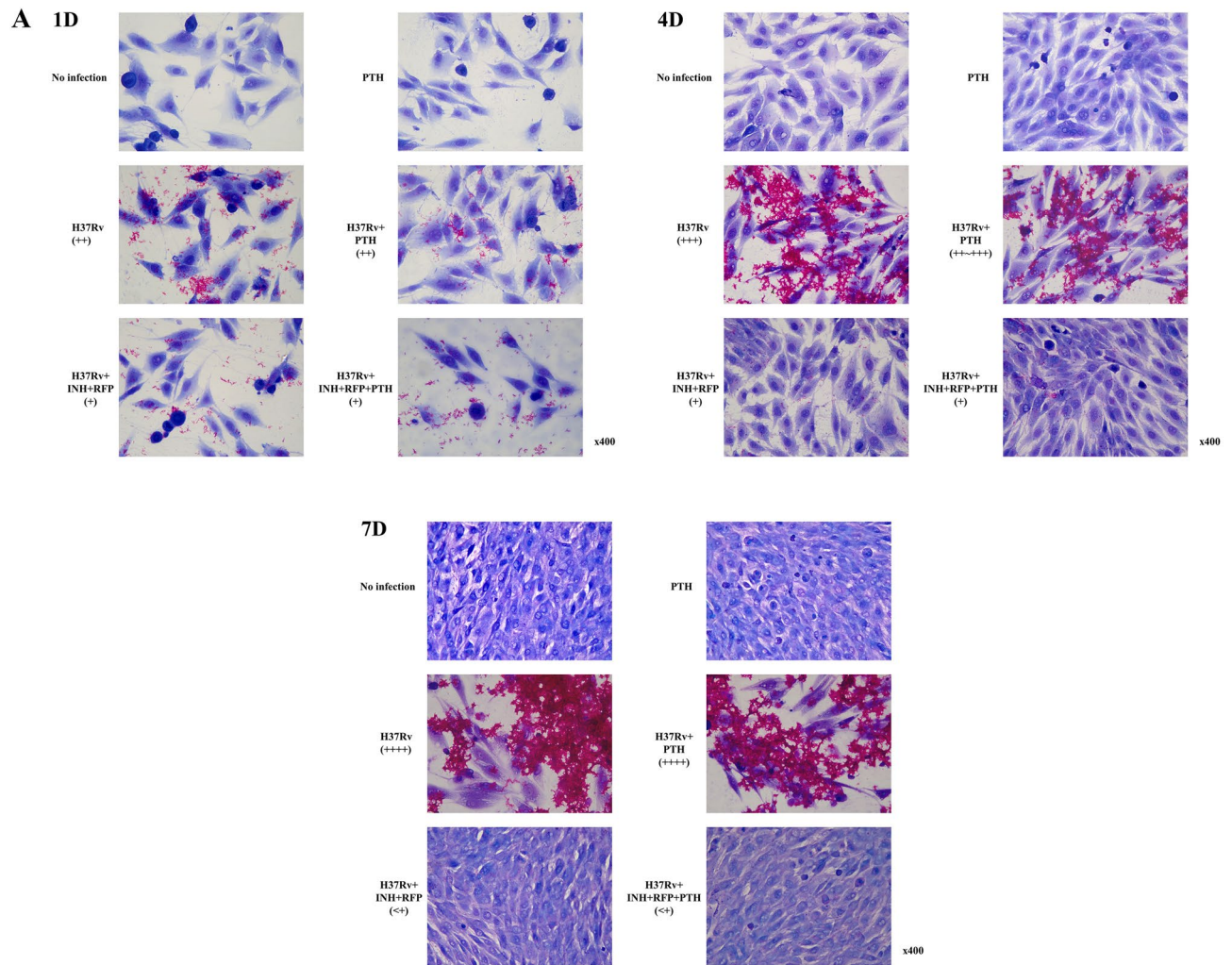
Effects of teriparatide on Mtb-infected MG-63 Cells. After several preliminary experiments, we identified that the effective dosing protocol for determining the optimal activity of teriparatide against MG-63 cell proliferation was intermittent exposure to the drug. We changed the differentiation medium after treatment with 400 ng/mL teriparatide for only 4 h every 48 h. The result of the alkaline phosphatase (ALP) and alizarin red S (ARS) staining obtained following this protocol showed that teriparatide enhanced the osteoblastic function with or without eradicating Mtb.

The ALP staining results on day 7 showed that eradication of Mtb with INH + RFP increased the ALP-positive area induced by teriparatide treatment by 705%, from 0.95 ± 0.34 to 6.70 ± 1.16 ($P=0.0031$). The ALP positive area was higher following cotreatment with teriparatide and the anti-tuberculosis drugs (teriparatide with INH + RFP: 6.70 ± 1.16 , $P=0.0116$) than it was with teriparatide alone (2.24 ± 0.45). The ALP-positive area increased by 299%, from 2.24 to 6.70, by INH and RFP under the same teriparatide dosing condition (Table 2, Fig. 3A).

The ARS staining results on day 28 showed that teriparatide treatment increased the positively stained area of uninfected MG-63 cells (control) by 2015%, from 0.20 ± 0.07 to 4.03 ± 1.46 ($P=0.0398$). The results of the control group in this study confirmed the validity of our ARS experimental protocol for evaluating the effect of teriparatide on MG63, and showed that it promoted osteogenesis.

The non-specific staining of Mtb and MG-63 cell necrosis indicated that the ARS-positive area was larger 28 days after Mtb infection progressed than it was in the absence of Mtb infection (Control: 0.20 ± 0.07 , H37Rv: 6.68 ± 1.56 , $P=0.006$). Thus, the effect of teriparatide was investigated using the same protocol used for the control and the ARS staining was performed under Mtb infection conditions. Teriparatide treatment increased the ARS-positive area of Mtb-infected MG-63 cells by 326%, from 6.68 ± 1.56 to 21.80 ± 2.90 ($P=0.0037$), and it effectively promoted osteogenesis in Mtb-infected MG-63 cells without Mtb eradication (Table 3, Fig. 3B).

Regulation of chemokine secretion in Mtb-infected MG-63 Cells. The levels of chemokines secreted following Mtb infection were measured and the results showed that teriparatide did not significantly affect secretion levels of the four chemokines investigated. These results suggest that teriparatide did not affect the inflammatory level of Mtb-infected osteoblasts. The levels of IL-8 and MCP-1 showed no difference among the experimental groups and were independent of the presence or absence of Mtb infection or administration of the anti-tuberculosis drugs and teriparatide. In contrast, Mtb infection induced significantly higher levels of IP-10 and RANTES than those of the uninfected group on days 4 and 7, whereas the anti-tuberculosis drugs significantly reduced these levels compared to those of the untreated group (Table 4, Fig. 4).



B * The number of Mtb bacilli (CFU)

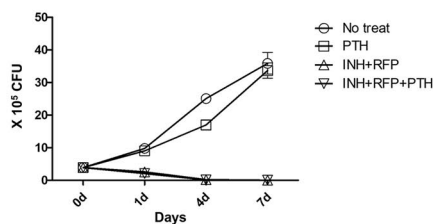


Figure 2. Microscopic images of acid fast bacillus (AFB) and Giemsa staining results. (A) +: < 500 bacilli, ++: 500–1000 bacilli, +++: 1000–3000 bacilli, ++++: > 3000 bacilli). 400× magnification. (B) CFU results. (A), 1 day after drug administration (1D). Anti-tuberculosis drugs showed slight inhibitory effect on Mtb growth, 4 days after drug administration (4D). Growth of Mtb increased, and anti-tuberculosis drugs significantly inhibited Mtb activity. No apparent difference was observed in osteoblast density according to concentration of teriparatide administered, 7 days after drug administration (7D). Significant proliferation of osteoblasts was evident. Mtb proliferation was significantly increased in the absence of anti-tuberculosis drugs. Anti-tuberculosis drugs completely inhibited bacterial growth. No apparent difference was observed in osteoblast density according to teriparatide administration; (B), CFU results by time point. Mtb activity of infected MG-63 increased four-fold for 7 days. Mtb was eradicated by anti-tuberculosis drug. Teriparatide did not affect Mtb activity. Abbreviations: AFB, acid-fast bacilli; CFU, colony-forming units; INH, isoniazid; PTH, teriparatide; RFP, rifampin; Mtb, *Mycobacterium tuberculosis*.

ALP-positive area (%)	H37Rv	H37Rv + PTH	H37Rv + INH + RFP	H37Rv + INH + RFP + PTH
Test 1	2.12	1.84	4.10	6.04
Test 2	0.65	1.96	2.19	8.04
Test 3	0.60	1.38	1.09	3.27
Test 4	0.42	3.76	4.72	9.45
AVE	0.95	2.24	3.03	6.70
SEM	0.34	0.45	0.73	1.16
<i>P</i> -value (vs H37Rv)		0.0637	0.0415	0.0031
<i>P</i> -value (vs H37Rv + PTH)			0.3923	0.0116
<i>P</i> -value (vs H37Rv + INF + RFP)				0.0364

Table 2. Alkaline phosphatase (ALP) staining results.

Discussion

To the best of our knowledge, the effectiveness of cotreatment with anti-tuberculosis agents and teriparatide has not been investigated, and therefore, we aimed to examine this phenomenon in this study. First, our *in vitro* study revealed that teriparatide did not affect the efficacy of anti-tuberculosis drugs. Second, we established an *in vitro* model of Mtb infected osteoblast using H37rv with MG-63, and demonstrated that teriparatide did not increase the rate of Mtb infection. In addition, we verified that teriparatide treatment increased the anabolic bone effect in infected and uninfected (control) osteoblasts.

Clinicians have implemented anti-tuberculosis drugs as the first-line therapy for spondylitis treatment. Furthermore, eradication of Mtb using anti-tuberculosis agents is the most important factor to restore the osteogenic ability of infected osteoblasts. The first requirement for teriparatide to ensure its suitability for use in combination therapy is that it should not reduce the effectiveness of the anti-tuberculosis drugs. The *in vitro* resazurin MIC method showed that teriparatide did not adversely affect the anti-tuberculous effect of INH and RFP, which eliminated concerns about drug–drug interactions.

The data on optimal drug regimens and duration for tuberculous spondylitis treatment are limited because of drug-resistant Mtb. However, an observational study showed that spinal lesions contain fewer bacilli than do pulmonary lesions and are less likely to have drug-resistant mutants⁹. The two-drug regimen of only INH and RFP in combination was used in this study, based on the design of two previously reported randomized controlled trials for tuberculous spondylitis treatment^{10,11}. Clinical trials of the short chemotherapy course for tuberculous spondylitis in Hong Kong, India, and South Korea reported that regimens using INH and RFP produced comparable results with those that used INH with either ethambutol or para-aminosalicylic acid¹¹.

The recombinant human PTH analog teriparatide was approved in 2002 by the US Food and Drug Administration (FDA) for the treatment of osteoporosis at high risk for fracture and increased bone mass in postmenopausal women¹². This drug has been demonstrated to promote bone healing and prevent fragility fractures in both rats and humans^{13,14}. In addition to its numerous clinical advantages, teriparatide has some less well-known contraindications, such as a history of radiation therapy¹⁵, the presence of primary malignant and metastatic bone tumors^{7,16}, and Paget's disease¹⁷. As tuberculous spondylitis might also be a contraindicated comorbidity, targeted experiments to determine whether teriparatide enhances infection and inflammation induced by Mtb infection is expedient. In the present study, we showed that teriparatide did not increase the activity of Mtb based on the CFU analysis of the infected MG-63 cell line. Furthermore, the ELISA results revealed that teriparatide lacked regulatory effects on the selected chemokines known to be related to changes in bone metabolism due to osteomyelitis or bone tumor. This observation indicated that teriparatide was not associated with changes in inflammation of the Mtb-infected osteoblasts.

In vivo production of chemokines during human Mtb infection is well documented^{18,19}. However, studies of osteoblasts in osteomyelitis are relatively few. We evaluated some chemokines with the most established role in physiological and pathological bone remodeling²⁰. For inflammatory osteomyelitis, stimulation with tumor necrosis factor (TNF)- α and IL-1 β has shown that osteoblasts secrete IL-8²¹, MCP-1^{22,23}, and IP-10²⁴. Our results showed that IL-8 and MCP-1 were increased under all conditions regardless of Mtb infection and their levels peaked on day 4 after infection, followed by a decrease on day 7. Mtb infection did not contribute to increasing levels of the two inflammatory chemokines, IL-8 and MCP-1. A role for IL-8 in bone metastatic disease was demonstrated in studies with breast cancer cells^{25,26}. Osteoblasts and osteoclasts were shown to express IL-8 following stimulation with inflammatory mediators²⁷. IL-8 stimulates bone resorption and could act as an essential regulatory signal for pathological bone remodeling. Moreover, the pro-inflammatory chemokine MCP-1, which plays a crucial role in bone remodeling²⁸, was shown to be involved in several pathological conditions. For instance, MCP-1 contributed to bone metastasis development in cancers such as multiple myeloma²⁹, prostate cancer³⁰, oral squamous cell carcinoma³¹, and breast cancer³². MCP-1 increases tumor growth and bone metastasis by recruiting macrophages and osteoclasts to the tumor site³³. Moreover, inflammatory mediators or bacteria were found to induce the expression of MCP-1 by osteoblasts *in vivo*^{34,35}, which contributed to inflammatory bone loss. In our experiment, IL-8 and MCP-1 did not increase specifically with Mtb infection; therefore, a difference in chemokine expression likely exists between the diseases mentioned above and tuberculous spondylitis.

In contrast, the secretion of IP-10 and RANTES, which were specifically increased by Mtb infection, significantly decreased after anti-tuberculous drug treatment. Numerous studies attempted to characterize the

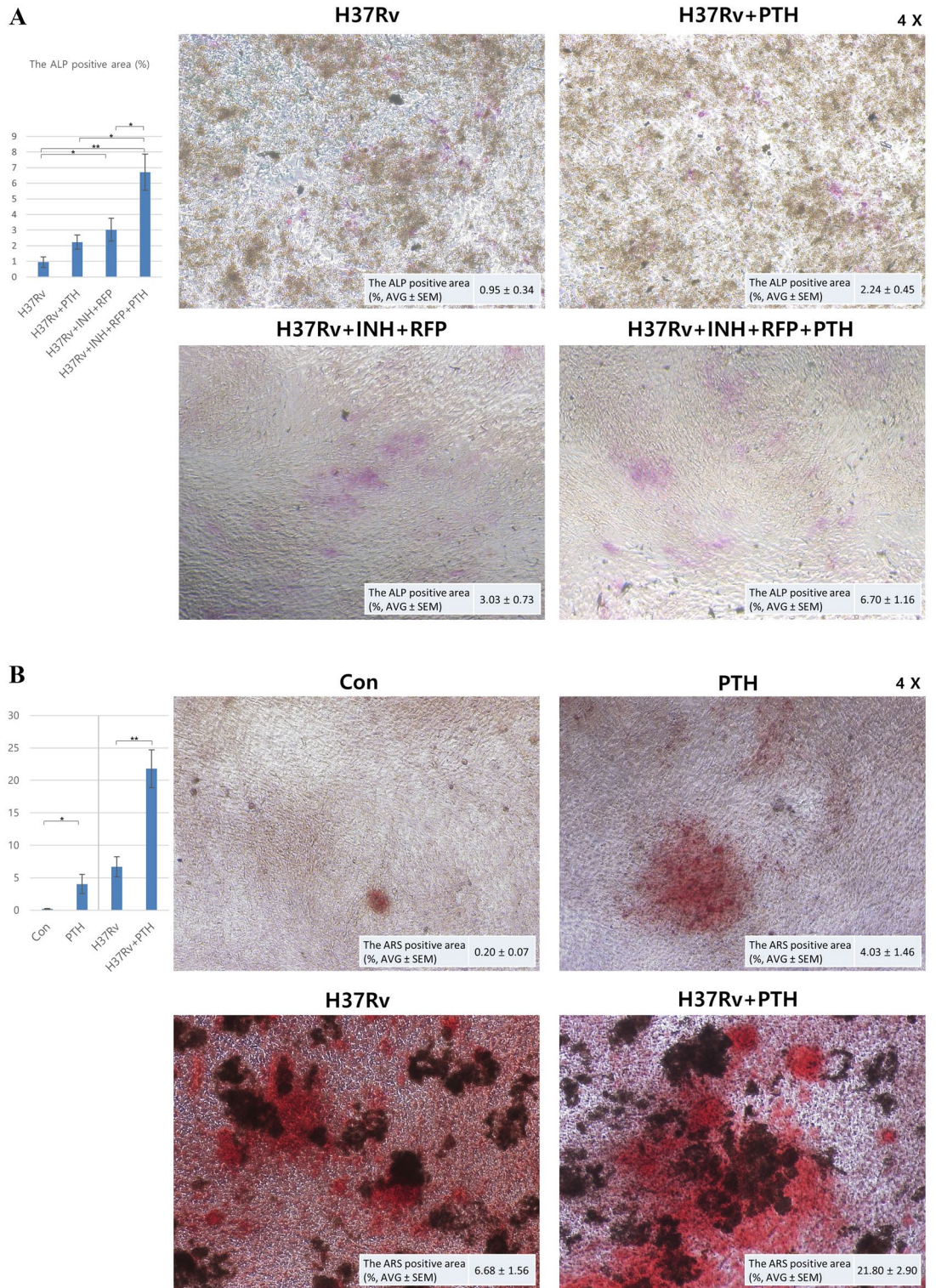


Figure 3. Alkaline phosphatase (ALP) and alizarin red S (ARS). (A) ALP- and (B) ARS-positive area was measured using bioquantification software (Bioquant Osteo II, R&M Biometrics, Nashville, TN, USA), and graphs show comparison of positive area for each group. Abbreviations: AVG, average; Con, control; INH, isoniazid; PTH, teriparatide; RFP, rifampin; SEM, standard error of mean; * $P < 0.05$; ** $P < 0.01$.

expression of chemokines in response to Mtb in vitro and in vivo, in human and murine systems. However, synthesizing an understanding of cell infiltration and granuloma formation using results from these descriptive studies has proved difficult³⁶. Human macrophages produced RANTES in response to virulent stains of

ARS-positive area (%)	Control	PTH	H37Rv	H37Rv + PTH
Test 1	0.23	1.41	5.04	21.41
Test 2	0.06	0.81	5.75	15.91
Test 3	0.09	7.07	11.97	31.26
Test 4	0.40	6.83	3.97	18.61
AVE	0.20	4.03	6.68	21.80
SEM	0.07	1.46	1.56	2.90
P value (vs Con)		0.0398	0.006	0.0003
P value (vs PTH)			0.2612	0.0016
P value (vs H37Rv)				0.0037

Table 3. Alizarin red S (ARS) staining result.

	No (Control)						PTH						H37Rv					
	1	2	3	4	AVE	SEM	1	2	3	4	AVE	SEM	1	2	3	4	AVE	SEM
IL-8(pg/ml)																		
Day 0	151.1	144	120.6		138.57	9.21	151.1	144	120.6		138.57	9.21	142.3	147	132.7		140.67	4.21
Day 1	206.7	197.3	325.6	319.1	262.18	34.82	205.7	199.4	337.9	339.9	270.73	39.38	232.7	231.5	329.6	324.2	279.50	27.39
Day 4	364.6	377.1	402.5	419.2	390.85	12.31	386.7	360.2	419.7	394.9	390.38	12.26	362.4	350.4	405	395.6	378.35	13.05
Day 7	367.6	348.6	373.6	361.6	362.85	5.34	350.4	338.2	385.7	361.6	358.98	10.11	208.8	210	337.5	349.5	276.45	38.79
MCP-1(pg/ml)																		
Day 0	163.07	178.25	302.2		214.51	44.07	163.07	178.25	302.2		214.51	44.07	150.57	159.05	297.6		202.41	47.66
Day 1	503.34	520.36	345.3	359.1	432.03	46.30	551.13	501.88	351.7	349.4	438.53	51.78	530.75	531.68	328.6	316	426.76	60.36
Day 4	729.34	694.11	698.7	706.3	707.11	7.82	730.95	707.52	655.1	667.8	690.34	17.55	477.29	475.77	669.2	682.5	576.19	57.60
Day 7	550.77	515.54	587.7	549.5	550.88	14.74	552.38	528.95	614.7	609.6	576.41	21.21	298.71	297.2	688.9	676.6	490.35	111.11
IP-10(pg/ml)																		
Day 0	3	2.4	4.5		3.30	0.62	3	2.4	4.5		3.30	0.62	2.5	2.9	5		3.47	0.78
Day 1	2.6	4.9	5	6.4	4.73	0.79	1.2	2	7.5	7.3	4.50	1.68	10.4	6.2	5.2	3.9	6.43	1.41
Day 4	24.7	24.6	33.5	40.1	30.73	3.76	25.3	28.3	40.3	38.9	33.20	3.76	1021.4	1025.8	1683.9	1593	1331.03	178.46
Day 7	353.4	359.3	488	494.6	423.83	39.00	401.6	394.1	494.8	493.5	446.00	27.84	1460.9	1467.8	2087.5	1995.3	1752.88	167.65
RANTES(pg/ml)																		
Day 0	0	0	0	0	0.00	0.00	0	0	0	0	0.00	0.00	0	0	0	0	0.00	0.00
Day 1	0	0	0	0	0.00	0.00	0	0	0	0	0.00	0.00	0	0	0	0	0.00	0.00
Day 4	0	0	0	0	0.00	0.00	0	0	0	0	0.00	0.00	139.6	123.9	0	0	65.88	38.17
Day 7	555.2	526.3	277.14	255.12	403.44	79.62	611.7	622.8	243.36	282.86	440.18	102.57	952.3	920.4	764.5	786.77	855.99	47.07
H37Rv + PTH																		
H37Rv + INH + RFP																		
H37Rv + INH + RFP + PTH																		
	1	2	3	4	AVE	SEM	1	2	3	4	AVE	SEM	1	2	3	4	AVE	SEM
IL-8(pg/ml)																		
Day 0	142.3	147	132.7		140.67	4.21	142.3	147	132.7		140.67	4.21	142.3	147	132.7		140.67	4.21
Day 1	200.2	205.2	320.9	349.1	268.85	38.64	188.8	185	324.3	330	257.03	40.51	198.6	193.3	302.3	303.6	249.45	30.91
Day 4	338.3	362.4	387.4	395.3	370.85	12.92	339.9	346	408.8	411.8	376.63	19.49	342.2	359.9	424	423	387.28	21.23
Day 7	211.9	208.8	325.4	325.4	267.88	33.22	205.6	205.7	313.4	301.3	256.50	29.46	186.3	197.5	301.3	337.5	255.65	37.61
MCP-1(pg/ml)																		
Day 0	150.57	159.05	297.6		202.41	47.66	150.57	159.05	297.6		202.41	47.66	150.57	159.05	297.6		202.41	47.66
Day 1	500.34	547.88	347.4	347.2	435.71	51.95	472.71	499.11	317	333.2	405.51	46.85	482.21	466.48	371.4	360.5	420.15	31.53
Day 4	501.57	494.55	662.4	674.3	583.21	49.24	489.07	481.98	644	628.2	560.81	43.61	469.09	495.73	685	685	583.71	58.73
Day 7	323	315.98	695.9	637.5	493.10	100.95	310.5	303.41	623.2	586	455.78	86.27	290.52	317.16	679.3	667.4	488.60	106.83
IP-10(pg/ml)																		
Day 0	2.5	2.9	5		3.47	0.78	2.5	2.9	5		3.47	0.78	2.5	2.9	5		3.47	0.78
Day 1	17.1	10.2	4.3	4.4	9.00	3.03	9	11.4	5.3	7.5	8.30	1.28	4.8	5.6	3	6.2	4.90	0.70
Day 4	1252.7	1249.1	1865.7	1956.6	1581.03	191.50	196.3	195.7	264.4	261.1	229.38	19.28	155	155.9	247.4	237.6	198.98	25.21
Day 7	1412.8	1410.1	2257.6	2353.4	1858.48	258.83	937.9	909.1	718.9	715.6	820.38	59.83	908.4	931.8	701.9	692.2	808.58	64.60
RANTES(pg/ml)																		
Day 0	0	0	0	0	0.00	0.00	0	0	0	0	0.00	0.00	0	0	0	0	0.00	0.00
Day 1	0	0	0	0	0.00	0.00	0	0	0	0	0.00	0.00	0	0	0	0	0.00	0.00
Day 4	127.6	120.9	0	0	62.13	35.89	332	321.3	0	0	163.33	94.32	262.2	263	0	0	131.30	75.81
Day 7	927.1	872.2	845.5	737.86	845.67	39.75	635.4	605.1	321	317.32	469.71	87.14	532.4	493.6	310.5	264.47	400.24	66.25

Table 4. Enzyme-linked immunosorbent assay (ELISA) of inflammatory chemokines. IL-8, interleukin-8; IP-10, interferon γ -induced protein 10 kDa; MCP-1, monocyte chemoattractant protein-1; RANTES, regulated upon activation, normal T cell expressed and presumably secreted.

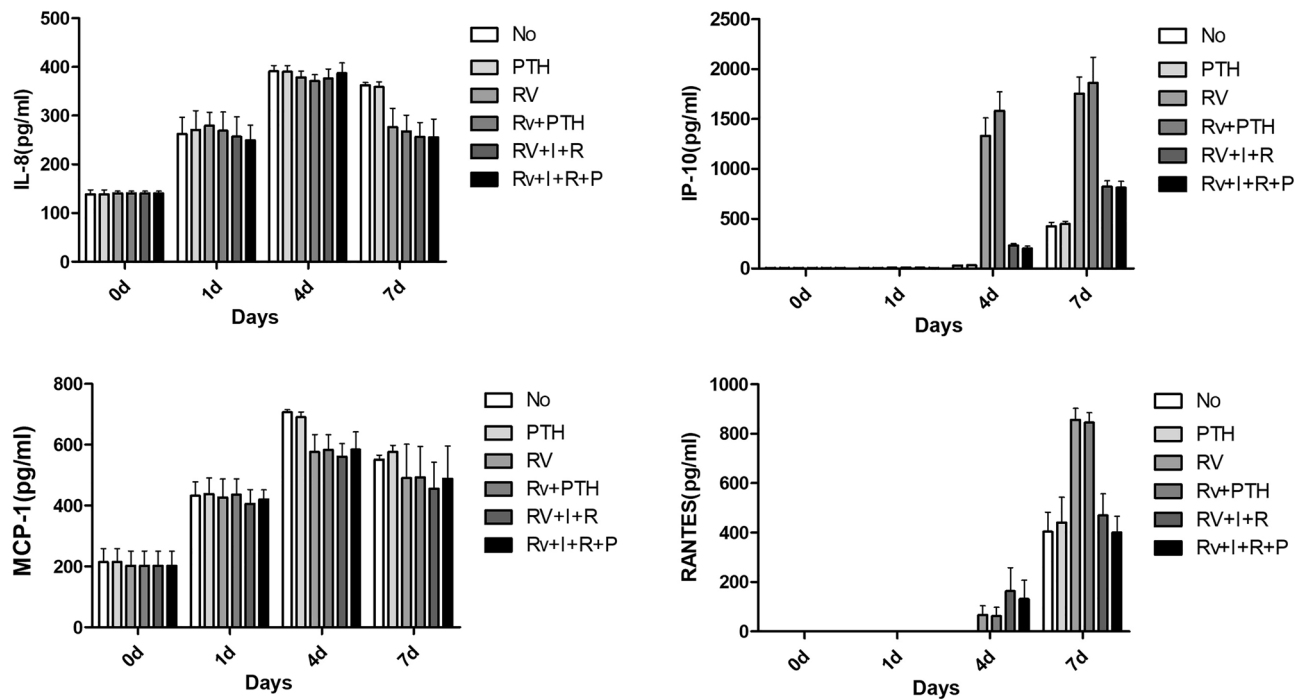


Figure 4. Enzyme-linked immunosorbent assay (ELISA) results of four representative chemokines related to pathologic inflammatory conditions in osteoblasts. Abbreviations: INH, isoniazid; IL-8, interleukin-8; IP-10, interferon γ -induced protein-10; MCP-1, monocyte chemoattractant protein-1; P, teriparatide; PTH, teriparatide; RIF, rifampin; RANTES, regulated upon activation normal, T cell expressed and presumably secreted; RV, *Mycobacterium tuberculosis* H37RV strain infection.

*M. tuberculosis*³⁷. Studies performed using bronchoalveolar lavage fluid indicate elevated levels of RANTES and IP-10 in tuberculosis patients compared to uninfected controls^{38–40}. Expression of IP-10 in response to *M. tuberculosis* infection in mice has been reported^{41,42}.

Previous studies suggest that RANTES is involved in the pathological progression of rheumatoid arthritis, osteoarthritis, osteomyelitis, and posttraumatic responses^{43,44}. RANTES, along with other β -chemokines, has been shown to induce osteoclast chemotaxis⁴⁵. IP-10 also promotes osteoclastic differentiation and osteolysis⁴⁶, and impacts pathological bone remodeling in osteoporosis⁴⁷, bone metastasis⁴⁸, and rheumatoid arthritis⁴⁹. The results of this study showed that the pathological microenvironment of tuberculous spondylitis could include RANTES and IP-10. Furthermore, IP-10 and RANTES are secreted later than MCP-1 and may be associated with delayed recruitment and activation of T lymphocytes during inflammation⁴³. T lymphocyte recruitment is essential for granuloma development, and the production of IP-10 may be necessary for mediating the establishment of the type 1 cytokine profile observed in tuberculosis¹⁸.

Teriparatide has been widely demonstrated to reduce the risk of osteoporotic vertebral compression fractures. The primary motivation for this study was also the possibility of lowering the fracture risk of infectious spondylitis. Vertebral bodies of infectious spondylitis patients exhibit osteolytic change. A Japanese orthopedic surgeon, Shinohara, reported that vertebral body erosion was rapidly restored in pyogenic spondylitis by teriparatide therapy⁵⁰. However, this was an off-label use of this agent without any evidence to support its usefulness in spondylitis.

Debilitating spontaneous destruction of bone and consequent severe spinal deformity are typical clinical courses of tuberculous spondylitis. In a clinical trial, teriparatide showed an effect on fracture healing⁵¹. Moreover, animal studies on fracture models have shown that the addition of teriparatide promotes fracture healing^{52,53}. Compared to previously reported pathologic conditions such as severe osteoporosis, trauma, or pyogenic spondylitis, *Mtb* infection is a much more unfavorable microenvironment for bone healing. Surgical treatment is inevitable in cases where fracture healing fails and spinal deformity with neurologic deterioration eventually occurs. However, the success rate of complete bone fusion during anti-tuberculosis treatment could be unsatisfactory^{6,10}. Teriparatide has the potential to improve the osteointegration outcome of spondylitis surgeries. Although in non-infectious conditions, multiple studies had indicated that daily administration of teriparatide might promote osseous union in patients with osteoporosis undergoing posterior fusion with or without interbody support^{54,55}.

In addition, Kuroshima et al. reported positive effects of teriparatide in preventing osteonecrosis in rats administered bisphosphonates and steroids⁵⁶. Moreover, osteoblasts were considerably increased and osteoclasts and necrotic bone were decreased by teriparatide treatment after bisphosphonates and steroid use⁵⁶. Teriparatide had a positive impact on the resolution of the inflammatory response of bone healing, but the mechanism of action of teriparatide is unknown⁵⁷.

The prevailing view for many years has been that osteoclasts do not express PTH receptors and that PTH's effects on osteoclasts are mediated indirectly via osteoblasts⁵⁸. However, teriparatide may have a direct effect on

osteoclasts which reduces the bone resorption rate^{58,59}. In addition, teriparatide reduce inflammatory cytokines, so it is likely to inhibit osteoclast-mediated bone resorption. In addition, teriparatide had an inhibitory effect on several types of acute inflammation, reported previously⁶⁰. Dohke et al. demonstrated that teriparatide rapidly and significantly inhibited the expression of inflammatory cytokines, such as IL-1 β , IL-6, and TNF- α in an OVX mouse model⁶¹. Inhibition of these inflammatory cytokines by teriparatide may have the effect of reducing the osteoclast differentiation. According to these studies, we estimate that the total amount of bone formation will be positive, even including bone resorption by osteoclasts.

Since osteoclast activity is increased in Mtb-infected Ob, the inhibition effect of inflammatory cytokines by teriparatide may have an adjuvant action to alleviate bone destruction in tuberculous spondylitis. Moreover, Mtb powder lysed by ultrasound significantly enhanced osteoclast formation, bone absorption, and facilitate secretion of TNF- α and IFN- γ . Furthermore, it significantly increased mRNA expression of receptor activator of nuclear factor κ -B ligand (RANKL) in osteoblast and simultaneously decreased osteoprotegerin (OPG) expression, thus decreasing OPG/RANKL ratio⁶². OPG is an antagonist to osteoclast differentiation and inhibits the RANKL/RANK signaling pathway by binding to RANKL⁶³.

To prove that teriparatide has an anabolic effect on bone under Mtb-infected osteoblasts, we used ALP and ARS staining methods. ALP staining was performed on the 7th day and ARS staining was used to detect the mineralization nodules on the 28th day after differentiation⁶⁴. Using INH-RFP and teriparatide combination treatment, 705% ($P=0.0031$) of osteogenesis promotion was achieved compared to the no-treatment group in the ALP staining. In the ARS staining, 326% ($P=0.0037$) of osteogenesis promotion was achieved through teriparatide administration. Based on the present study, we expect teriparatide to improve the clinical outcome by reducing the risk of vertebral fractures with Mtb infection and increasing the success rate of both conservative and surgical treatment.

This study has several limitations that are worth mentioning. First, in the MIC test, we arbitrarily determined the dose of teriparatide without any experimental or clinical evidence. The experimental concentrations used should be extrapolated based on the dose to be used in humans. Second, although we showed that teriparatide improved osteoblastic function in an in vitro tuberculous spondylitis model, only bioquantification software was used in the evaluation without statistical analysis. The software used might have been insufficient for the high level of evidence of osteogenic activation of infected osteoblasts. Third, osteoblast culture under various environments would be required for more meaningful conclusions. Future studies should investigate the microscopic changes in osteoblasts under an infectious environment using a lower Mtb MOI than that used in this study or only the exudate secreted by Mtb should be treated. Culturing infected osteoblasts directly from a patient with tuberculous spondylitis should also be considered. Fourth, although osteoclasts have an important role in tuberculous spondylitis, we did not investigate osteoclasts in this study, mainly because they lack receptors for teriparatide. Consequently, our experiments in this study were performed only with osteoblasts. Further studies would be necessary to analyze the osteoblast-osteoclast coupling chemokines, RANKL, osteoprotegerin, and granulocyte colony-stimulating factor (G-CSF). Co-culture of both osteoblasts and osteoclasts would also be helpful in providing additional information. Fifth, drugs other than teriparatide, which have bone formation effects, were not evaluated in the present study. In contrast to teriparatide, denosumab is an anti-resorptive agent that reduces the development and activity of osteoclasts by inhibiting the RANKL signaling pathway. Moreover, romosozumab is a bone-forming agent that inhibits sclerostin to promote bone formation and suppress bone resorption through a so-called “dual-effect”^{65,66}. These molecular-targeted drugs are prominent in the field of osteoporosis treatment⁶⁶. It is necessary to compare the effectiveness of each drug for tuberculous spondylitis in future study.

In conclusion, the target of tuberculous spondylitis treatment is elimination of the source of infection by administering anti-tuberculosis drugs. Moreover, adding a bone anabolic agent to alleviate bone destruction should also be considered. Thus, we sought to establish an experimental rationale for cotreatment with anti-tuberculosis drugs and teriparatide. We found that teriparatide did not affect the efficacy of anti-tuberculosis drugs and had no adverse effect on the progression of Mtb infection in osteoblasts. Furthermore, it did not change the expression of osteoblastic inflammatory chemokines. Finally, we showed that the intrinsic osteogenesis-promoting activity of teriparatide was maintained even in Mtb-infected osteoblasts and these results might serve as additional compelling evidence to support the potential usefulness of cotreatment with anti-tuberculous drugs and teriparatide in tuberculous spondylitis.

Methods

Experimental design. This study had two primary objectives (Fig. 5). First, we investigated whether teriparatide reduces the efficacy of anti-tuberculosis drugs. To this end, we used the virulent Mtb H37Rv strain (American Type Culture Collection [ATCC] 27,294; ATCC, Manassas, VA, USA) to evaluate the minimum inhibitory concentration (MIC) of the two most widely prescribed standard anti-tuberculosis agents, isoniazid (INH) and rifampin (RFP). This assay was conducted using the resazurin MIC method.

Second, an in vitro model of tuberculous spondylitis was established by infecting the human osteoblastic MG-63 cell line (KCLB no. 21427, Korean Cell Line Bank, Seoul, South Korea) with the Mtb H37Rv strain. This model was subsequently used to examine the effect of teriparatide on the infectious activity of Mtb. Levels of several chemokines were also measured using the enzyme-linked immunosorbent assay (ELISA). Finally, we evaluated the osteogenesis-promoting activity of teriparatide on Mtb-infected osteoblasts using alkaline phosphatase (ALP) and alizarin red S (ARS) staining.

Resazurin MIC method. For INH and RFP (catalog nos. I3377 and R3501, respectively; Sigma-Aldrich, St. Louis, MO, USA), the drug powder samples were dissolved in distilled water (DW) and methanol, respectively,

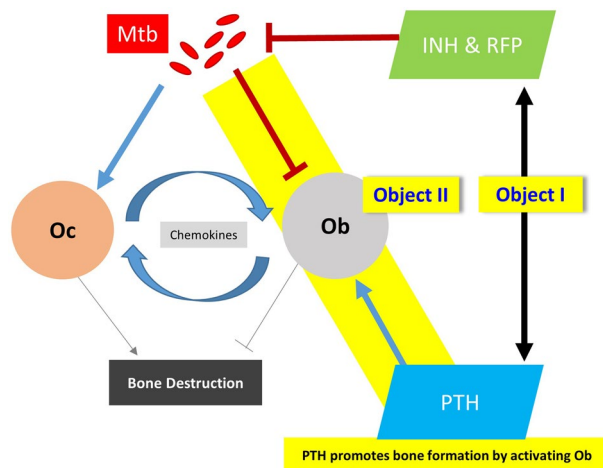


Figure 5. Schematic diagram of experimental design. Study objective was to address two questions to provide essential evidence to support the usefulness of teriparatide in patients with tuberculous spondylitis in clinical practice. Abbreviations: INH, isoniazid; Mtb, *Mycobacterium tuberculosis*; Ob, Osteoblast; Oc, Osteoclast; PTH, teriparatide; RFP, rifampin.

well ID	1	2	3	4	5	6	7	8	9	10	11	12
A												
B	INH +RFP (±PTH)	Serial two-fold dilution of drug									Mtb (positive)	
C												
D												
E	Serial two-fold dilution of drug									Media (negative)		
F												
G												
H												

Figure 6. Image of 96-well plate (Corning® 96 Well TC-Treated Microplates, Sigma-Aldrich, St. Louis, MO, USA) for resazurin minimum inhibitory concentration (MIC) assay method. Abbreviations: INH, isoniazid; Mtb, *Mycobacterium tuberculosis*; PTH, teriparatide; RFP, rifampin.

to a concentration of 0.5 mg/mL and stored at -20°C . Teriparatide (Eli Lilly and Company, Indianapolis, IN, USA) was dissolved in DW to a 5 $\mu\text{g}/\text{mL}$ solution and stored at -20°C . Resazurin sodium salt (catalog no. R7017; Sigma-Aldrich, St. Louis, MO, USA) was dissolved in DW to a concentration of 0.025% immediately before the experiment. The Mtb H37Rv strain was cultured for 2 weeks in Middlebrook 7H9 broth containing 10% oleic albumin dextrose catalase (OADC), 0.5% glycerol, and 0.05% Tween 80 (Sigma-Aldrich, St. Louis, MO, USA).

The test was performed as follows: (1) Culture medium (100 μL) was placed in a 96-well plate (Corning® 96 Well TC-Treated microplates; Sigma-Aldrich, St. Louis, MO, USA). (2) Then, μL each of 32 $\mu\text{g}/\text{mL}$ RFP and 3.2 $\mu\text{g}/\text{mL}$ INH solutions were added to the top well to obtain final concentrations of 4 $\mu\text{g}/\text{mL}$ RFP and 0.4 $\mu\text{g}/\text{mL}$ INH, followed by a twofold serial dilution. (3) Then, 100 μL bacterial solution was diluted to an optical density (OD) 0.01/mL. The Mtb bacilli were incubated with the anti-tuberculosis drugs for 10 days to establish the MIC in this experiment. (4) Predesignated wells were treated with teriparatide at concentrations of 50, 100, and 250 ng/mL. (5) The plates were wrapped in foil and incubated for 1 week in 5% CO_2 incubator at 37°C . (6) After treatment with 20 μL of a 0.025% resazurin solution, the plates were incubated for 2 more days. (7) Finally, color development was examined and confirmed in the plates to determine the growth status of the cells: pink and blue, growth or no growth of Mtb, respectively (Fig. 6).

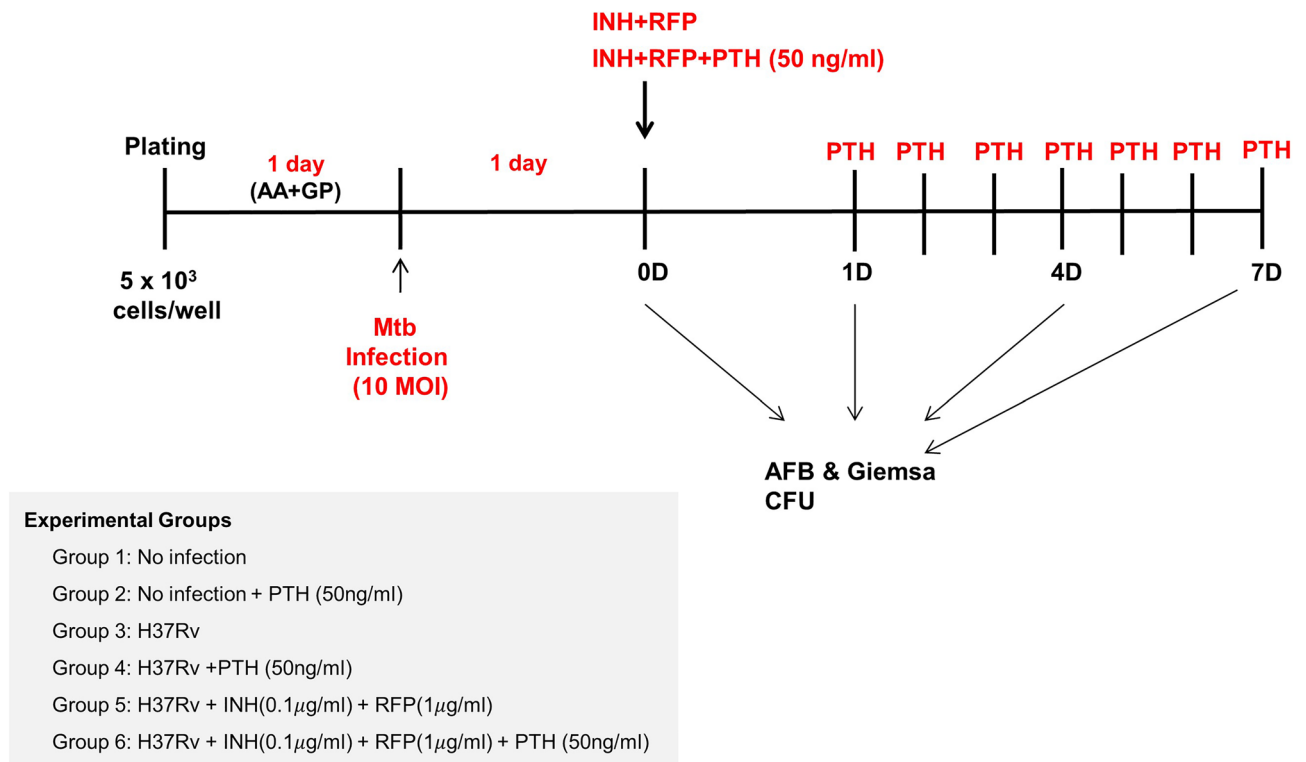


Figure 7. Experimental protocol for infecting MG-63 osteoblasts with *Mycobacterium tuberculosis* (Mtb) and cotreatment of cells with anti-tuberculosis drugs and teriparatide. Abbreviations: AA, ascorbic acid; AFB, acid-fast bacilli; CFU, colony-forming units; FACS, fluorescence-activated cell sorting; GP, β-glycerophosphate; INH, isoniazid; PTH, teriparatide; RFP, rifampin.

MG-63 osteoblast culture. The human osteoblastic MG-63 cell line was obtained from the Korean Cell Line Bank (KCLB no. 21427) and maintained in Dulbecco's modified Eagle's medium ([DMEM]/high glucose; HyClone, Logan, UT, USA) supplemented with 10% fetal bovine serum (FBS; HyClone, Morningside, QLD, Australia) and 1% penicillin and streptomycin (P/S; Gibco, Invitrogen Corporation, Carlsbad, CA, USA) in a humidified 5% CO₂ atmosphere at 37 °C. The MG-63 cells were trypsinized with 0.25% trypsin (HyClone, Logan, UT, USA), seeded, finally cultured for 48 h at an appropriate density, and were used when they achieved 90% confluence.

Mtb H37Rv strain culture. The Mtb H37Rv strain was maintained in Middlebrook 7H9 medium with Tween 80, albumin, and glycerol for 14 days at 37 °C in an atmosphere of 5% CO₂.

Mtb-infected osteoblast: an in vitro model. MG-63 cells were plated at a density of 5×10^3 cells/well on medium mixed with DMEM, 10% FBS, ascorbic acid (50 μg/mL), and β-glycerophosphate (10 mM) and incubated for 24 h. The cells were transfected with the Mtb H37Rv strain at a rate of 10 multiplicity of infection (MOI), incubated overnight, and then each group was treated with the anti-tuberculosis drugs (INH and RFP) and teriparatide (50 ng/mL). On day 1, 4, and 7 post treatment, acid-fast bacilli (AFB) and Giemsa staining were performed. The established in vitro Mtb-infected MG-63 cell model was evaluated using colony-forming units (CFU) assessment (Fig. 7).

Osteogenic activity of Mtb-infected osteoblasts. The preliminary experiment identified the teriparatide treatment protocol that induced the highest increase in osteoblastic activity of the MG-63 cells, which is shown in Fig. 8A. The cells were treated with teriparatide 400 ng/mL every 48 h, incubated for 4 h, washed, and then the culture medium was replaced. For ALP staining, MG-63 cells were plated at a density of 1×10^5 cells/well with 10 MOI Mtb on medium and the Stem TAG™ ALP staining kit (Cell Biolabs, San Diego, CA, USA) was used to measure the ALP activity on day 4 and 7 post treatment (Fig. 8A).

ARS staining was performed to quantify the mineralized bone nodules, as another marker for osteoblastic activity. Briefly, cells were treated with teriparatide for 28 days and because of the overgrowth of Mtb and MG-63 cells, the cell numbers and MOI were reduced to 5×10^3 cells/well and 0.1 MOI, respectively (Fig. 8B). The number of red nodules observed with ARS staining was counted under a microscope. The stained wells were quantified using a microscope interfaced with a digital camera and a bioquantification software system (Bioquant Osteo II, R&M Biometrics, Nashville, TN, USA) using a previously described method⁶⁷. We confirmed the effect of teriparatide treatment on bone volume/tissue volume ratio using a bioquantification analysis software.

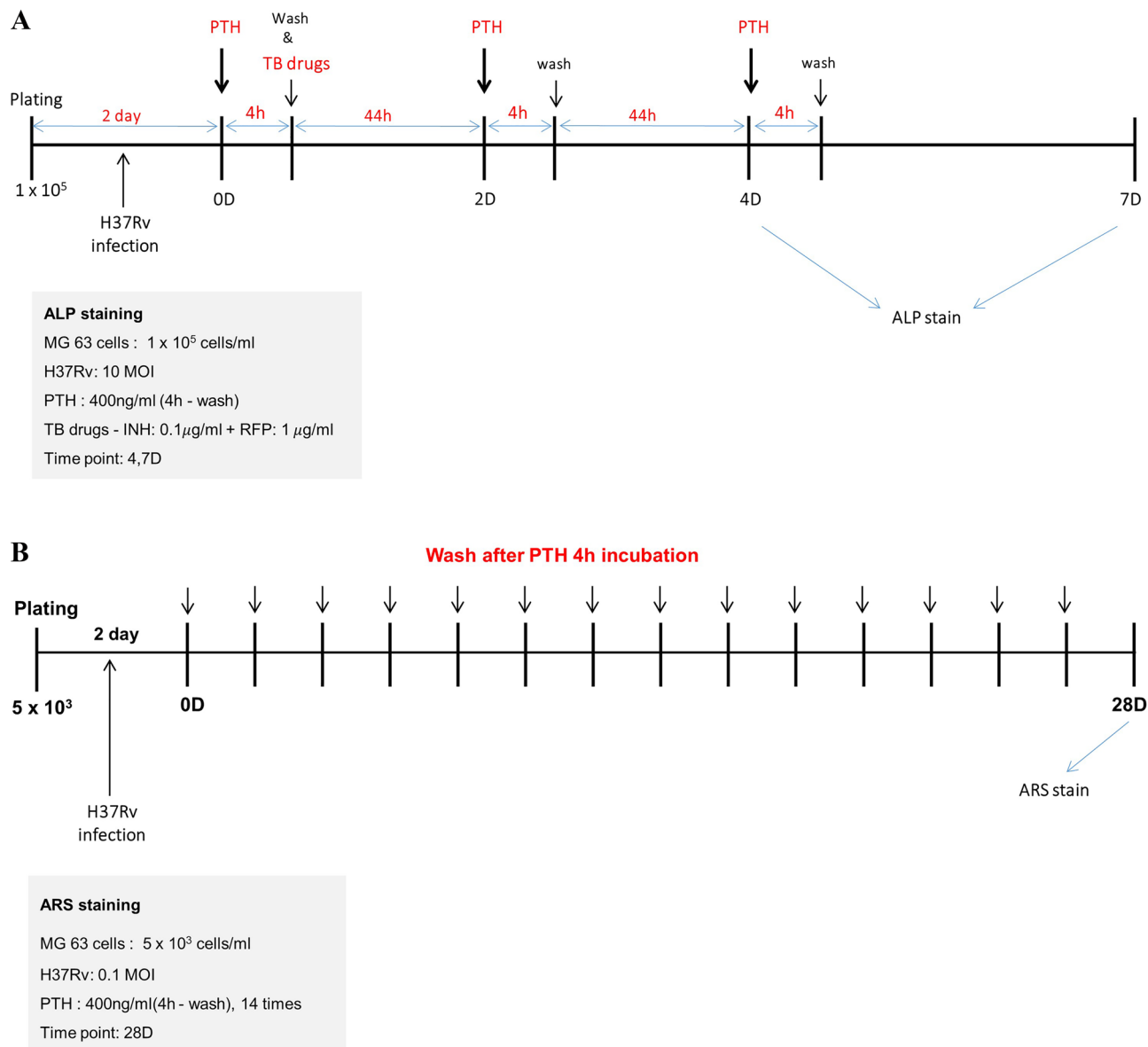


Figure 8. Experimental protocol for measuring osteoblastic activity of *Mycobacterium tuberculosis* (Mtb)-infected MG-63 cells. **(A)** ALP and **(B)** ARS staining. Abbreviations: ALP, alkaline phosphatase; ARS, Alizarin red S; INH, isoniazid; MOI, multiplicity of infection; PTH, teriparatide; RFP, rifampin; TB, anti-tuberculosis.

Bone volume was defined as the ALP- and ARS (bone nodule area)-positive areas in the ALP and ARS staining assays, respectively.

Elisa. Culture supernatants were harvested at each time point shown in Fig. 7, passed through a $0.2 \mu\text{m}$ spin filter to remove viable organisms, and frozen before assaying for chemokine proteins. The levels of interleukin (IL-8), monocyte chemoattractant protein-1 (MCP-1), interferon γ -induced protein 10 kDa (IP-10), and regulated upon activation normal, T cell expressed and presumably secreted (RANTES) were detected using ELISA with matched pairs of antibodies (R&D Systems, Minneapolis, MN, USA) according to the manufacturer's instructions. The lower limit of sensitivity of the IP-10 assay was 11 pg/mL and that of all other ELISAs was 3 pg/mL . The results are expressed as picogram per milliliters (pg/mL) and are presented as means \pm standard error of the mean (SEM) of at least three experiments.

Data availability

Upon request by e-mail to the corresponding author, we (including all co-authors) will confirm the use and provide research materials.

Received: 25 July 2022; Accepted: 25 November 2022

Published online: 15 December 2022

References

1. WHO. Global Tuberculosis Report 2020. World Health Organization, Geneva, Switzerland, (2020).
2. Lacerda, C., Linhas, R. & Duarte, R. Tuberculous spondylitis: A report of different clinical scenarios and literature update. *Case Rep. Med.* **2017**, 4165301. <https://doi.org/10.1155/2017/4165301> (2017).
3. Peto, H. M., Pratt, R. H., Harrington, T. A., LoBue, P. A. & Armstrong, L. R. Epidemiology of extrapulmonary tuberculosis in the United States, 1993–2006. *Clin. Infect. Dis.* **49**, 1350–1357. <https://doi.org/10.1086/605559> (2009).
4. Colmenero, J. D. *et al.* Pyogenic, tuberculous, and brucellar vertebral osteomyelitis: A descriptive and comparative study of 219 cases. *Ann. Rheum. Dis.* **56**, 709–715. <https://doi.org/10.1136/ard.56.12.709> (1997).
5. Jain, A. K. Tuberculosis of the spine. *J. Bone Joint Surg. British* **92 B**, 905–913. <https://doi.org/10.1302/0301-620x.92b7.24668> (2010).
6. Rahyussalim, A. J. *et al.* New bone formation in tuberculous-infected vertebral body defect after administration of bone marrow stromal cells in rabbit model. *Asian Spine J.* **10**, 1–5. <https://doi.org/10.4184/asj.2016.10.1.1> (2016).
7. Koski, A.-M., Sikiö, A. & Forslund, T. Teriparatide treatment complicated by malignant myeloma. *BMJ Case Rep.* <https://doi.org/10.1136/bcr.01.2010.2681> (2010).
8. Hodsman, A. B. *et al.* Parathyroid hormone and teriparatide for the treatment of osteoporosis: A review of the evidence and suggested guidelines for its use. *Endocr. Rev.* **26**, 688–703. <https://doi.org/10.1210/er.2004-0006> (2005).
9. Debeaumont, A. Bactériologie de la tuberculose ostéoarticulaire sous chimiothérapie. *Advances Tuberc. Res.* **15**, 125 (1966).
10. Controlled trial of short-course regimens of chemotherapy in the ambulatory treatment of spinal tuberculosis. Results at three years of a study in Korea. Twelfth report of the medical research council working party on tuberculosis of the spine. *J. Bone Joint Surg Br* **75**, 240–248. <https://doi.org/10.1302/0301-620x.75b2.8444944> (1993).
11. Darbyshire, J. Five-year assessment of controlled trials of short-course chemotherapy regimens of 6, 9 or 18 months duration for spinal tuberculosis in patients ambulatory from the start or undergoing radical surgery. *Int. Orthop.* **23**, 73–81. <https://doi.org/10.1007/s002640050311> (1999).
12. Gilsenan, A. *et al.* Long-term cancer surveillance: Results from the forteo patient registry surveillance study. *Osteoporos. Int.* **32**, 645–651. <https://doi.org/10.1007/s00198-020-05718-0> (2021).
13. Alkhiary, Y. M. *et al.* Enhancement of experimental fracture-healing by systemic administration of recombinant human parathyroid hormone (PTH 1–34). *JBJS* **87**, 731–741. <https://doi.org/10.2106/jbjs.D.02115> (2005).
14. Neer, R. M. *et al.* Effect of parathyroid hormone (1–34) on fractures and bone mineral density in postmenopausal women with osteoporosis. *N. Engl. J. Med.* **344**, 1434–1441. <https://doi.org/10.1056/nejm200105103441904> (2001).
15. Subbiah, V., Madsen, V. S., Raymond, A. K., Benjamin, R. S. & Ludwig, J. A. Of mice and men: Divergent risks of teriparatide-induced osteosarcoma. *Osteoporos. Int.* **21**, 1041–1045. <https://doi.org/10.1007/s00198-009-1004-0> (2010).
16. Harper, K. D., Kregel, J. H., Marcus, R. & Mitlak, B. H. Osteosarcoma and teriparatide?. *J. Bone Miner. Res.* **22**, 334–334. <https://doi.org/10.1359/jbmr.061111> (2007).
17. Andrews, E. B. *et al.* The US postmarketing surveillance study of adult osteosarcoma and teriparatide: Study design and findings from the first 7 years. *J. Bone Miner. Res.* **27**, 2429–2437. <https://doi.org/10.1002/jbmr.1768> (2012).
18. Barnes, P. F. *et al.* Cytokine production at the site of disease in human tuberculosis. *Infect. Immun.* **61**, 3482–3489. <https://doi.org/10.1128/iai.61.8.3482-3489.1993> (1993).
19. Lin, Y., Gong, J., Zhang, M., Xue, W. & Barnes, P. F. Production of monocyte chemoattractant protein 1 in tuberculosis patients. *Infect Immun.* **66**, 2319–2322. <https://doi.org/10.1128/iai.66.5.2319-2322.1998> (1998).
20. Brylka, L. J. & Schinke, T. Chemokines in physiological and pathological bone remodeling. *Front. Immunol.* **10**, 2182 (2019).
21. Chaudhary, L. R. & Avioli, L. V. Dexamethasone regulates IL-1 beta and TNF-alpha-induced interleukin-8 production in human bone marrow stromal and osteoblast-like cells. *Calcif. Tissue Int.* **55**, 16–20. <https://doi.org/10.1007/bf00310163> (1994).
22. Zhu, J. F., Valente, A. J., Lorenzo, J. A., Carnes, D. & Graves, D. T. Expression of monocyte chemoattractant protein 1 in human osteoblastic cells stimulated by proinflammatory mediators. *J. Bone Miner. Res.* **9**, 1123–1130. <https://doi.org/10.1002/jbmr.5650090721> (1994).
23. Posner, L. J. *et al.* Monocyte chemoattractant protein-1 induces monocyte recruitment that is associated with an increase in numbers of osteoblasts. *Bone* **21**, 321–327. [https://doi.org/10.1016/s8756-3282\(97\)00154-3](https://doi.org/10.1016/s8756-3282(97)00154-3) (1997).
24. Proost, P. *et al.* Identification of a novel granulocyte chemotactic protein (GCP-2) from human tumor cells In vitro and in vivo comparison with natural forms of GRO, IP-10, and IL-8. *J. Immunol.* **150**, 1000–1010 (1993).
25. Bendre, M., Gaddy, D., Nicholas, R. W. & Suva, L. J. Breast cancer metastasis to bone: It is not all about PTHrP. *Clin. Orthop. Relat. Res.* <https://doi.org/10.1097/01.blo.0000093844.72468.f4> (2003).
26. Kamalakar, A. *et al.* Circulating interleukin-8 levels explain breast cancer osteolysis in mice and humans. *Bone* **61**, 176–185. <https://doi.org/10.1016/j.bone.2014.01.015> (2014).
27. Rothe, L. *et al.* Human osteoclasts and osteoclast-like cells synthesize and release high basal and inflammatory stimulated levels of the potent chemokine interleukin-8. *Endocrinology* **139**, 4353–4363. <https://doi.org/10.1210/endo.139.10.6247> (1998).
28. Sul, O. J. *et al.* Absence of MCP-1 leads to elevated bone mass via impaired actin ring formation. *J. Cell Physiol.* **227**, 1619–1627. <https://doi.org/10.1002/jcp.22879> (2012).
29. Moreaux, J. *et al.* Osteoclast-gene expression profiling reveals osteoclast-derived CCR2 chemokines promoting myeloma cell migration. *Blood* **117**, 1280–1290. <https://doi.org/10.1182/blood-2010-04-279760> (2011).
30. Lu, Y. *et al.* Monocyte chemotactic protein-1 (MCP-1) acts as a paracrine and autocrine factor for prostate cancer growth and invasion. *Prostate* **66**, 1311–1318. <https://doi.org/10.1002/pros.20464> (2006).
31. Quan, J., Morrison, N. A., Johnson, N. W. & Gao, J. MCP-1 as a potential target to inhibit the bone invasion by oral squamous cell carcinoma. *J. Cell Biochem.* **115**, 1787–1798. <https://doi.org/10.1002/jcb.24849> (2014).
32. Molloy, A. P. *et al.* Mesenchymal stem cell secretion of chemokines during differentiation into osteoblasts, and their potential role in mediating interactions with breast cancer cells. *Int. J. Cancer* **124**, 326–332. <https://doi.org/10.1002/ijc.23939> (2009).
33. Mizutani, K. *et al.* The chemokine CCL2 increases prostate tumor growth and bone metastasis through macrophage and osteoclast recruitment. *Neoplasia* **11**, 1235–1242. <https://doi.org/10.1593/neo.09988> (2009).
34. Marriott, I. *et al.* Osteoblasts produce monocyte chemoattractant protein-1 in a murine model of *Staphylococcus aureus* osteomyelitis and infected human bone tissue. *Bone* **37**, 504–512. <https://doi.org/10.1016/j.bone.2005.05.011> (2005).
35. Rahimi, P. *et al.* Monocyte chemoattractant protein-1 expression and monocyte recruitment in osseous inflammation in the mouse. *Endocrinology* **136**, 2752–2759. <https://doi.org/10.1210/endo.136.6.7750500> (1995).
36. Algood, H. M. S., Chan, J. & Flynn, J. L. Chemokines and tuberculosis. *Cytokine Growth Factor Rev.* **14**, 467–477. [https://doi.org/10.1016/S1359-6101\(03\)00054-6](https://doi.org/10.1016/S1359-6101(03)00054-6) (2003).
37. Saukkonen, J. J. *et al.* β -Chemokines are induced by mycobacterium tuberculosis and inhibit its growth. *Infect. Immun.* **70**, 1684–1693 (2002).
38. Kurashima, K. *et al.* Elevated chemokine levels in bronchoalveolar lavage fluid of tuberculosis patients. *Am. J. Respir. Crit. Care Med.* **155**, 1474–1477 (1997).
39. Miotto, D. *et al.* Expression of IFN- γ -inducible protein; Monocyte chemotactic proteins 1, 3, and 4; and eotaxin in TH1- and TH2-mediated lung diseases. *J. Allergy Clin. Immunol.* **107**, 664–670 (2001).
40. Sadek, M. I., Sada, E., Toossi, Z., Schwander, S. K. & Rich, E. A. Chemokines induced by infection of mononuclear phagocytes with mycobacteria and present in lung alveoli during active pulmonary tuberculosis. *Am. J. Respir. Cell Mol. Biol.* **19**, 513–521 (1998).

41. Scott, H. M. & Flynn, J. L. Mycobacterium tuberculosis in chemokine receptor 2-deficient mice: Influence of dose on disease progression. *Infect. Immun.* **70**, 5946–5954 (2002).
42. Peters, W. *et al.* Chemokine receptor 2 serves an early and essential role in resistance to Mycobacterium tuberculosis. *Proc. Natl. Acad. Sci.* **98**, 7958–7963 (2001).
43. Wright, K. M. & Friedland, J. S. Differential regulation of chemokine secretion in tuberculous and staphylococcal osteomyelitis. *J. Bone Miner. Res.* **17**, 1680–1690. <https://doi.org/10.1359/jbmr.2002.17.9.1680> (2002).
44. Lisignoli, G. *et al.* Different chemokines are expressed in human arthritic bone biopsies: IFN-gamma and IL-6 differently modulate IL-8, MCP-1 and rantes production by arthritic osteoblasts. *Cytokine* **20**, 231–238. <https://doi.org/10.1006/cyto.2002.2006> (2002).
45. Yu, X., Huang, Y., Collin-Osdoby, P. & Osdoby, P. CCR1 chemokines promote the chemotactic recruitment, RANKL development, and motility of osteoclasts and are induced by inflammatory cytokines in osteoblasts. *J. Bone Miner. Res.* **19**, 2065–2077. <https://doi.org/10.1359/jbmr.040910> (2004).
46. Lee, J.-H. *et al.* CXCL10 promotes osteolytic bone metastasis by enhancing cancer outgrowth and osteoclastogenesis. *Can. Res.* **72**, 3175. <https://doi.org/10.1158/0008-5472.CAN-12-0481> (2012).
47. Müller, A. *et al.* Involvement of chemokine receptors in breast cancer metastasis. *Nature* **410**, 50–56. <https://doi.org/10.1038/35065016> (2001).
48. Zlotnik, A., Burkhardt, A. M. & Homey, B. Homeostatic chemokine receptors and organ-specific metastasis. *Nat. Rev. Immunol.* **11**, 597–606. <https://doi.org/10.1038/nri3049> (2011).
49. Kwak, H. B. *et al.* Reciprocal cross-talk between RANKL and interferon-gamma-inducible protein 10 is responsible for bone-erosive experimental arthritis. *Arthritis Rheum.* **58**, 1332–1342. <https://doi.org/10.1002/art.23372> (2008).
50. Shinohara, A., Ueno, Y. & Marumo, K. Weekly teriparatide therapy rapidly accelerates bone healing in pyogenic spondylitis with severe osteoporosis. *Asian Spine J.* **8**, 498–501. <https://doi.org/10.4184/asj.2014.8.4.498> (2014).
51. Aspenberg, P. & Johansson, T. Teriparatide improves early callus formation in distal radial fractures. *Acta Orthop.* **81**, 234–236. <https://doi.org/10.3109/17453671003761946> (2010).
52. Pietrogrande, L. & Raimondo, E. Teriparatide in the treatment of non-unions: Scientific and clinical evidences. *Injury* **44**, S54–S57. [https://doi.org/10.1016/S0020-1383\(13\)70013-5](https://doi.org/10.1016/S0020-1383(13)70013-5) (2013).
53. Barvencik, F. Medication and bone metabolism: Clinical importance for fracture treatment. *Unfallchirurg* **118**, 1017–1024. <https://doi.org/10.1007/s00113-015-0109-5> (2015).
54. Ohtori, S. *et al.* Teriparatide accelerates lumbar posterolateral fusion in women with postmenopausal osteoporosis prospective study. *Spine* **37**, 1464–1468. <https://doi.org/10.1097/BRS.0b013e31826ca2a8> (2012).
55. Cho, P. G. *et al.* An effect comparison of teriparatide and bisphosphonate on posterior lumbar interbody fusion in patients with osteoporosis: A prospective cohort study and preliminary data. *Eur. Spine J.* **26**, 691–697. <https://doi.org/10.1007/s00586-015-4342-y> (2017).
56. Kuroshima, S., Entezami, P., McCauley, L. & Yamashita, J. Early effects of parathyroid hormone on bisphosphonate/steroid-associated compromised osseous wound healing. *Osteoporos. Int.* **25**, 1141–1150 (2014).
57. Keskinruzgar, A. *et al.* Histopathological effects of teriparatide in medication-related osteonecrosis of the jaw: An animal study. *J. Oral Maxillofac. Surg.* **74**, 68–78. <https://doi.org/10.1016/j.joms.2015.07.005> (2016).
58. Dempster, D. W. *et al.* Normal human osteoclasts formed from peripheral blood monocytes express PTH type 1 receptors and are stimulated by PTH in the absence of osteoblasts. *J. Cell. Biochem.* **95**, 139–148. <https://doi.org/10.1002/jcb.20388> (2005).
59. Glover, S. J. *et al.* Rapid and robust response of biochemical markers of bone formation to teriparatide therapy. *Bone* **45**, 1053–1058. <https://doi.org/10.1016/j.bone.2009.07.091> (2009).
60. Caruso, A. *et al.* Parathyroid hormone fragment 1–34 inhibits drug-induced inflammation in various experimental models. *Eur. J. Pharmacol.* **198**, 85–88 (1991).
61. Dohke, T. *et al.* Teriparatide rapidly improves pain-like behavior in ovariectomized mice in association with the downregulation of inflammatory cytokine expression. *J. Bone Miner. Metab.* **36**, 499–507. <https://doi.org/10.1007/s00774-017-0865-0> (2018).
62. Li, Z. *et al.* The role of TNF- α and IFN- γ in the formation of osteoclasts and bone absorption in bone tuberculosis. *Int. J. Clin. Exp. Pathol.* **9**, 8406–8414 (2016).
63. Simonet, W. *et al.* Osteoprotegerin: A novel secreted protein involved in the regulation of bone density. *Cell* **89**, 309–319 (1997).
64. Luo, Y. *et al.* MicroRNA-224 suppresses osteoblast differentiation by inhibiting SMAD4. *J. Cell. Physiol.* **233**, 6929–6937. <https://doi.org/10.1002/jcp.26596> (2018).
65. Ominsky, M. S. *et al.* Differential temporal effects of sclerostin antibody and parathyroid hormone on cancellous and cortical bone and quantitative differences in effects on the osteoblast lineage in young intact rats. *Bone* **81**, 380–391 (2015).
66. Kobayakawa, T. *et al.* Denosumab versus romosozumab for postmenopausal osteoporosis treatment. *Sci. Rep.* **11**, 11801. <https://doi.org/10.1038/s41598-021-91248-6> (2021).
67. Al-Shatti, T., Barr, A. E., Safadi, F. F., Amin, M. & Barbe, M. F. Increase in inflammatory cytokines in median nerves in a rat model of repetitive motion injury. *J. Neuroimmunol.* **167**, 13–22. <https://doi.org/10.1016/j.jneuroim.2005.06.013> (2005).

Author contributions

S.L., J.Y.C., S.Y.E., and D.C.C. planned the experiments. Y.J.S., X.C., M.S.H., and S.K.L. performed processing of the investigation. S.L., and S.Y.E. wrote original draft preparation. J.Y.C., H.J.K., S.Y.E., and D.C.C. reviewed and edited the writing. S.L., X.C., M.S.H., S.K.L., and D.C.C. performed the data analysis. All authors have read and agreed to the published version of the manuscript.

Funding

This work was supported by Biomedical Research Institute grant, Kyungpook National University Hospital (2020).

Competing interests

The authors declare no competing interests.

Additional information

Correspondence and requests for materials should be addressed to D.-C.C.

Reprints and permissions information is available at www.nature.com/reprints.

Publisher's note Springer Nature remains neutral with regard to jurisdictional claims in published maps and institutional affiliations.



Open Access This article is licensed under a Creative Commons Attribution 4.0 International License, which permits use, sharing, adaptation, distribution and reproduction in any medium or format, as long as you give appropriate credit to the original author(s) and the source, provide a link to the Creative Commons licence, and indicate if changes were made. The images or other third party material in this article are included in the article's Creative Commons licence, unless indicated otherwise in a credit line to the material. If material is not included in the article's Creative Commons licence and your intended use is not permitted by statutory regulation or exceeds the permitted use, you will need to obtain permission directly from the copyright holder. To view a copy of this licence, visit <http://creativecommons.org/licenses/by/4.0/>.

© The Author(s) 2022